Atmos. Chem. Phys., 18, 11409–11422, 2018 https://doi.org/10.5194/acp-18-11409-2018 © Author(s) 2018. This work is distributed under the Creative Commons Attribution 4.0 License.





# Evaluation of OH and HO<sub>2</sub> concentrations and their budgets during photooxidation of 2-methyl-3-butene-2-ol (MBO) in the atmospheric simulation chamber SAPHIR

Anna Novelli<sup>1</sup>, Martin Kaminski<sup>1,a</sup>, Michael Rolletter<sup>1</sup>, Ismail-Hakki Acir<sup>1,b</sup>, Birger Bohn<sup>1</sup>, Hans-Peter Dorn<sup>1</sup>, Xin Li<sup>1,c</sup>, Anna Lutz<sup>2</sup>, Sascha Nehr<sup>1,d</sup>, Franz Rohrer<sup>1</sup>, Ralf Tillmann<sup>1</sup>, Robert Wegener<sup>1</sup>, Frank Holland<sup>1</sup>, Andreas Hofzumahaus<sup>1</sup>, Astrid Kiendler-Scharr<sup>1</sup>, Andreas Wahner<sup>1</sup>, and Hendrik Fuchs<sup>1</sup>

Correspondence: Anna Novelli (a.novelli@fz-juelich.de) and Hendrik Fuchs (h.fuchs@fz-juelich.de)

Received: 5 February 2018 – Discussion started: 14 March 2018

Revised: 18 July 2018 – Accepted: 31 July 2018 – Published: 15 August 2018

Abstract. Several previous field studies have reported unexpectedly large concentrations of hydroxyl and hydroperoxyl radicals (OH and HO<sub>2</sub>, respectively) in forested environments that could not be explained by the traditional oxidation mechanisms that largely underestimated the observations. These environments were characterized by large concentrations of biogenic volatile organic compounds (BVOC) and low nitrogen oxide concentration. In isoprene-dominated environments, models developed to simulate atmospheric photochemistry generally underestimated the observed OH radical concentrations. In contrast, HO<sub>2</sub> radical concentration showed large discrepancies with model simulations mainly in non-isoprene-dominated forested environments. An abundant BVOC emitted by lodgepole and ponderosa pines is 2methyl-3-butene-2-ol (MBO), observed in large concentrations for studies where the HO2 concentration was poorly described by model simulations. In this work, the photooxidation of MBO by OH was investigated for NO concentrations lower than 200 pptv in the atmospheric simulation chamber SAPHIR at Forschungszentrum Jülich. Measurements of OH and  $HO_2$  radicals, OH reactivity ( $k_{OH}$ ), MBO, OH precursors, and organic products (acetone and formaldehyde) were used to test our current understanding of the OH-oxidation mechanisms for MBO by comparing measurements with model calculations. All the measured trace gases agreed well with the model results (within 15 %) indicating a well understood mechanism for the MBO oxidation by OH. Therefore, the oxidation of MBO cannot contribute to reconciling the unexplained high OH and  $\rm HO_2$  radical concentrations found in previous field studies.

#### 1 Introduction

The hydroxyl radical (OH) is the most important daytime oxidant in the troposphere and its concentration affects the fate of many pollutants thus having a direct impact on the formation of ozone (O<sub>3</sub>) and oxygenated volatile organic compounds (OVOCs), and as such influencing particle formation and climate. Understanding the OH radical formation and destruction paths is therefore critical.

Measurements of OH radicals in environments characterized by low nitrogen oxide (NO) concentrations, pristine conditions, and isoprene being the most abundantly measured biogenic volatile organic compound (BVOC; Carslaw et al.,

<sup>&</sup>lt;sup>1</sup>Institute of Energy and Climate Research, IEK-8: Troposphere, Forschungszentrum Jülich GmbH, Jülich, Germany

<sup>&</sup>lt;sup>2</sup>Department of Chemistry and Molecular Biology, University of Gothenburg, Gothenburg, Sweden

<sup>&</sup>lt;sup>a</sup>now at: Bundesamt für Verbraucherschutz, Abteilung 5 – Methodenstandardisierung, Referenzlaboratorien und Antibiotikaresistenz, Berlin, Germany

<sup>&</sup>lt;sup>b</sup>now at: Institute of Nutrition and Food Sciences, Food Chemistry, University of Bonn, Bonn, Germany

<sup>&</sup>lt;sup>c</sup>now at: State Key Joint Laboratory of Environmental Simulation and Pollution Control, College of Environmental Sciences and Engineering, Peking University, Beijing, China

<sup>&</sup>lt;sup>d</sup>now at: INBUREX Consulting GmbH, Process Safety, Hamm, Germany

2001; Tan et al., 2001; Lelieveld et al., 2008; Whalley et al., 2011; Wolfe et al., 2011a), as well as in environments characterized by mixed emissions from biogenic and anthropogenic sources (Hofzumahaus et al., 2009; Lu et al., 2012, 2013; Tan et al., 2017), have shown a significant underestimation of observed OH concentrations by state-of-the-art models. In addition, the analysis of the OH budget using only measured species obtained by comparing all known OH radical sources together with the OH radical loss rate has demonstrated that the discrepancy with model simulations is due to a large missing OH radical source (Rohrer et al., 2014). Theoretical studies have proposed new OH recycling paths which, contrary to traditional mechanisms, do not require NO for the regeneration of HO<sub>x</sub> from RO<sub>2</sub> radicals. The proposed mechanism involves unimolecular reactions of specific isoprene peroxy radicals (RO<sub>2</sub>; Dibble, 2004; Peeters et al., 2009, 2014; Nguyen et al., 2010; Peeters and Müller, 2010; Silva et al., 2010; Peeters and Nguyen, 2012). Laboratory (Crounse et al., 2011) and chamber studies (Fuchs et al., 2013) have confirmed this mechanism and have helped with constraining its atmospheric impact. At the same time, other trace gases have been investigated as the results from the isoprene studies show that OH recycling through isoprene-RO2, alone, is not sufficient to explain the OH concentrations observed in the field. Chamber and laboratory studies on methacrolein (Crounse et al., 2012; Fuchs et al., 2014), methyl vinyl ketone (MVK; Praske et al., 2015), isoprene hydroxy hydroperoxide (D'Ambro et al., 2017), and glyoxal (Feierabend et al., 2008; Lockhart et al., 2013) - important products from the oxidation of isoprene by OH - have also shown new OH recycling paths as predicted by theory (Peeters et al., 2009; da Silva, 2010, 2012; Setokuchi, 2011). Further laboratory studies also have discovered OH radical recycling in the bimolecular reaction of HO<sub>2</sub> with acyl peroxy radicals which was previously considered to be a radical termination reaction only (Dillon and Crowley, 2008; Groß et al., 2014; Praske et al., 2015). These results underline the need to carefully investigate the OH radical budget, at least for the most abundant volatile organic compounds (VOCs), to test our current knowledge.

In a similar way, the  $\rm HO_2$  radical concentrations measured in several field campaigns performed in forested areas have shown measurement discrepancies with model calculations, highlighting an incomplete understanding of the chemistry involving formation and loss paths of  $\rm HO_2$  radicals. In some environments, the model tends to overestimate the measured  $\rm HO_2$  concentration (Stone et al., 2011), while in others there is the tendency to underestimate the measurements (Kubistin et al., 2010; Wolfe et al., 2011b, 2014; Hens et al., 2014). It has been recently shown that  $\rm HO_2$  radical measurements performed by laser-induced fluorescence (LIF) via conversion of  $\rm HO_2$  into OH after reaction with NO are likely affected by an interference that originates from organic peroxy radicals (Fuchs et al., 2011; Nehr et al., 2011; Whalley et al., 2013; Lew et al., 2018). Therefore some of the discrepancies

observed in previous studies may be partly caused by inaccurate HO2 radical measurements. Nevertheless, recent studies where this peroxy radical interference is accounted for still showed discrepancies with model calculations (Griffith et al., 2013; Hens et al., 2014; Wolfe et al., 2014). These recent studies, performed in environments where isoprene was not the dominantly measured BVOC, were all characterized by poor agreement between modelled and measured results for both OH and HO<sub>2</sub> concentrations, with the measurements being up to a factor of 3 higher than the model results. Good agreement was observed between modelled and measured OH radicals when the model is constrained to the HO<sub>2</sub> radical measurements. These studies have concluded that there is a missing HO<sub>2</sub> source for environments where the dominantly measured BVOCs are monoterpenes and 2-methyl-3-butene-2-ol (MBO; Hens et al., 2014; Wolfe et al., 2014). Corresponding photooxidation studies have been performed for  $\beta$ -pinene in the SAPHIR chamber at the Forschungszentrum Jülich. Consistent with field studies, a significant (up to a factor of 2) model underprediction of both OH and HO<sub>2</sub> concentrations was observed when  $\beta$ -pinene was oxidized by OH under low-NO conditions (< 300 pptv; Kaminski et al., 2017). The observed discrepancies in the chamber could be explained by additional HO<sub>2</sub> production, for which Kaminski et al. (2017) proposed a mechanism involving unimolecular radical reactions and photolysis of oxygenated products.

MBO is the dominant emission from lodgepole (Pinus Contorta) and ponderosa (Pinus Ponderosa) pines (Goldan et al., 1993; Harley et al., 1998). Its global emission is lower than that of isoprene (Guenther et al., 2012) but in forested areas within the western US, MBO is the most abundant BVOC measured contributing to most of the measured OH reactivity (Nakashima et al., 2014; Ortega et al., 2014). In the atmosphere, MBO reacts primarily with OH forming two peroxy radicals that yield acetone, glycolaldehyde, 2hydroxy-2-methylpropanal (HMPR), and formaldehyde after reaction with NO (Fantechi et al., 1998; Ferronato et al., 1998; Carrasco et al., 2006; Fig. 1). The reaction of the peroxy radicals with HO<sub>2</sub> yields two different dihydroxy hydroperoxides (MBOAOOH and MBOBOOH, Fig. 1). Recent theoretical studies have described a mechanism that involves additional hydrogen shift reactions for the RO<sub>2</sub> that reforms OH and produces HO<sub>2</sub> (Knap et al., 2015, 2016). As the predicted unimolecular reaction rate following the hydrogen shift is, at most,  $1.1 \times 10^{-3} \, \text{s}^{-1}$  (at 298 K and 1013 hPa) the study by Knap et al. (2016) concludes that in environments where the NO concentration is high (> 1 ppbv), the reaction between RO<sub>2</sub> and NO will be the dominant loss path for RO<sub>2</sub> radicals, and in forested areas, where the NO concentration is lower than 0.2 ppbv, reactions with HO<sub>2</sub> and RO<sub>2</sub> will dominate the RO<sub>2</sub> fate.

In this study, the photooxidation of MBO initiated by OH radicals is investigated in the atmospheric simulation chamber SAPHIR in the presence of approximately 200 pptv of NO. The OH and HO<sub>2</sub> budgets are analysed and a compari-

**Figure 1.** Simplified MBO OH-oxidation reaction scheme as described in the MCM version 3.3.1, including 1,4 and 1,5 H-shift reactions and their rate coefficients at 1013 hPa and 298 K as suggested by Knap et al. (2016). These H-shift reactions were added to the MCM version 3.3.1 kinetic model for a sensitivity test excluding the ones forming the epoxides (marked with the red crosses).

son with an up-to-date model is performed to test the current understanding of the oxidation processes of this important BVOC.

# 2 Methods

### 2.1 Atmospheric simulation chamber SAPHIR

The experiment performed in this study was conducted in the atmospheric simulation chamber SAPHIR at the Forschungszentrum Jülich, Germany. The chamber allows for the investigation of oxidation processes and mechanisms of organic compounds at atmospheric conditions in a controlled environment. The SAPHIR chamber has a cylindrical shape with a volume of 270 m<sup>3</sup> and is made of a double-walled Teflon (FEP) film that is inert and has a high transmittance for solar radiation (Bohn and Zilken, 2005). It is equipped with a shutter system that is opened during photol-

ysis experiments allowing the natural solar radiation to penetrate the chamber. The air provided to the chamber is mixed from ultra-pure nitrogen and oxygen (Linde, > 99.99990 %). A fan in the chamber ensures a complete mixing of trace gases within 2 minutes. The pressure in the chamber is slightly higher than ambient pressure ( $\sim 30\,\mathrm{Pa}$  higher) to avoid external air penetrating the chamber. Due to small leakages and air consumption by instruments, a dilution rate of  $\sim 4\,\%\,h^{-1}$  was required during this study. More details regarding the chamber can be found elsewhere (Rohrer et al., 2005; Poppe et al., 2007; Schlosser et al., 2007).

#### 2.2 Experimental procedure

At the beginning of the experiment, only synthetic air was present after flushing during the night. Evaporated Milli-Q<sup>®</sup> water was first introduced into the dark chamber by a carrier flow of synthetic air until a concentration of  $\sim 5 \times 10^{17}$  cm<sup>-3</sup>

	Taahnigua	Time resolution	1 ~ procision	1 ~ 000111001
	Technique	Time resolution	$1\sigma$ precision	$1\sigma$ accuracy
ОН	LIF	47 s	$0.3 \times 10^6  \text{cm}^{-3}$	13 %
OH	DOAS	200 s	$0.8 \times 10^6  \text{cm}^{-3}$	6.5 %
$HO_2$	LIF	47 s	$1.5 \times 10^7  \text{cm}^{-3}$	16 %
$k_{\mathrm{OH}}$	Laser-photolysis + LIF	180 s	$0.3  \mathrm{s}^{-1}$	10 %
NO	Chemiluminescence	180 s	4 pptv	5 %
$NO_2$	Chemiluminescence	180 s	2 pptv	5 %
HONO	LOPAP	300 s	1.3 pptv	12 %
$O_3$	UV-absorption	10 s	1 ppbv	5 %
MBO and Acetone	PTR-TOF-MS	30 s	> 15 pptv	< 14 %
MBO	GC	30 min	4-8 %	5 %
НСНО	Hantzsch monitor	120 s	20 pptv	5 %

**Table 1.** Instrumentation for radical and trace-gas quantification during the MBO oxidation experiment.

of water vapour was reached. Ozone produced by a silent discharge ozonizer (O3onia) was subsequently added to reach 40 pbbv in the chamber and was used to keep the concentration of NO within a few hundreds of pptv. This initial phase is defined as the dark phase. After opening the shutter system of the chamber, nitrous acid (HONO) was photochemically formed on the Teflon surface and released into the chamber. Its subsequent photolysis produced OH radicals and NO (Rohrer et al., 2005) during this so-called "zero-air" phase. Afterwards, the MBO was injected three times at intervals of about 2 hours using a high-concentration gas mixture of MBO ( $\sim 600$  ppm, 98 %, from Merck) premixed in a Silcosteel canister (Restek) to reach ~ 4 ppbv of MBO in the chamber after each injection. Two additional experiments where performed at very similar conditions but due to instrumental failures, they could not be included in this study. The experiment shown is composed of three independent injections of MBO and the range of NO and O<sub>3</sub> in the chamber is analogous to what was observed in the field studies where large concentrations of MBO were measured ( $\sim 50$  ppb of O<sub>3</sub> and 150 pptv of NO) giving confidence that what was observed in this study can be compared to ambient data.

#### 2.3 Instrumentation

Table 1 summarizes the instruments available during the experiment, quoting time resolution,  $1\sigma$  accuracy, and precision for each instrument. The concentrations of OH and  $HO_2$  radicals were measured with the LIF instrument permanently in use at the SAPHIR chamber and described previously (Holland et al., 2003; Fuchs et al., 2011). Recent studies have shown the possibility of interferences on the OH signal measured by LIF instruments that depend both on the chemical conditions of the sampled air and on the geometry of the different instruments (Mao et al., 2012; Novelli et al., 2014; Rickly and Stevens, 2018). A laboratory study performed with this LIF instrument (Fuchs et al., 2016) showed only interferences for high ozone concentrations (300–900 ppbv) together with BVOC concentra-

tions ranging from 1 to 450 ppbv, which are far beyond any condition encountered in this study. Therefore, the OH radical concentration measured by the LIF instrument in this study is considered free from interferences. In addition, OH was measured by differential optical absorption spectroscopy (DOAS; Dorn et al., 1995). Numerous intercomparisons between the LIF and the DOAS instrument in the SAPHIR chamber (Schlosser et al., 2007, 2009; Fuchs et al., 2012) showed very good agreement between these two instruments giving high reliability to the OH radical measurements performed in the chamber. OH concentration measurements by DOAS in this study were on average 14 % lower than those by LIF. This difference was well within the combined accuracies of measurements and was taken into account as additional uncertainty in OH concentration measurements in the analysis of this study, for which mainly OH data from the LIF instrument was used.

Several studies have proven that RO<sub>2</sub> radicals can cause an interference signal in the HO<sub>2</sub> radicals measured by conversion to OH after reaction with an excess of NO (Fuchs et al., 2011; Hornbrook et al., 2011; Whalley et al., 2013; Lew et al., 2018). It was shown that a reasonable approach for avoiding the interference is to lower the concentration of NO reacting with the sampled air inside the instrument. During this study, the NO concentration ( $\sim 2.5 \times 10^{13} \, \mathrm{cm}^{-3}$ ) was thus adjusted to lower the interference to a minimum as described in Fuchs et al. (2011). As during the investigation of the interference from RO<sub>2</sub> originating from the oxidation of different VOCs, MBO was not tested; the amount of interference that arises from its oxidation products is not known (Fuchs et al., 2011; Whalley et al., 2013; Lew et al., 2018). An upper limit could be estimated from experiments with isoprene peroxy radicals at similar operational conditions of the instrument. The relative detection sensitivity for RO<sub>2</sub> radicals originated from isoprene, compared to the HO<sub>2</sub> signal, was among the largest of the studied peroxy radical species, with a value of 20 % under the conditions of the present work (Fuchs et al., 2011). This value is considered to be a reasonable estimate bias in the HO<sub>2</sub> radical measurements and will be considered later in the discussion. The OH reactivity ( $k_{OH}$ ), the inverse lifetime of OH, was measured by a pump and probe technique coupled with a time-resolved detection of OH by LIF (Lou et al., 2010; Fuchs et al., 2017). MBO was measured by a proton-transfer-reaction time-of-flight mass spectrometer (PTR-TOF-MS; Lindinger et al., 1998; Jordan et al., 2009) and a gas chromatography system (GC; Wegener et al., 2007) with a PTR-TOF-MS to GC ratio of  $1.1\pm0.1$ , and acetone by PTR-TOF-MS. As the PTR-TOF-MS was calibrated only for the species listed above, concentrations for other species were not available. Formaldehyde (HCHO) was detected with a Hantzsch monitor (Kelly and Fortune, 1994); HONO with a long-path absorption photometry (LOPAP; Li et al., 2014); carbon monoxide (CO) with a reduction gas analysis instrument (RGA; Wegener et al., 2007); carbon dioxide (CO<sub>2</sub>), methane (CH<sub>4</sub>), and water vapour by an instrument applying cavity ring-down spectroscopy (CRDS; Picarro); NO and nitrogen dioxide (NO<sub>2</sub>) with chemiluminescence (CL; Ridley et al., 1992); and O<sub>3</sub> by UV absorption (Ansyco). Photolysis frequencies were calculated from measurements of solar actinic radiation by a spectroradiometer (Bohn et al., 2005; Bohn and Zilken, 2005).

#### 2.4 Model calculations

A zero-dimensional box model using chemical mechanistic information from the Master Chemical Mechanism, MCM version 3.3.1 (Jenkin et al., 1997; Saunders et al., 2003) downloaded via website: http://mcm.leeds.ac.uk/MCM (last access: February 2018) was used to calculate radical and trace gas concentrations. The model was implemented with specific chamber-related properties. First, a dilution rate was applied to all the trace gases present in the model to account for the dilution from the replenishing flow. The background production of HONO, HCHO, and acetone, known to occur in the sunlit chamber (Rohrer et al., 2005; Karl et al., 2006), was parameterized by an empirical function that depends on temperature, relative humidity, and solar radiation. Source strengths were adjusted to match the time series of HCHO and acetone during the zero-air phase, when the chamber was the only source for these species ( $\sim 0.3 \,\mathrm{ppbv}\,\mathrm{h}^{-1}$ ). These chamber sources also impacted the OH reactivity measured during the zero-air phase. Ideally, after accurately accounting for the chamber sources, the OH reactivity should be well represented by the model, but it is commonly the case that there is still the need for an OH reactant equivalent to  $\sim 1.0 \, \mathrm{s}^{-1}$  of OH reactivity. This unexplained reactivity is parameterized with a co-reactant Y added to the model, which converts OH to HO<sub>2</sub> in the same way as CO does (Fuchs et al., 2012, 2014; Kaminski et al., 2017). The concentration of Y was adjusted to match the observed OH reactivity during the zero-air phase of the experiment and was kept constant throughout the experiment. The uncertainty in the OH reactivity in this experiment was  $\pm 0.6 \,\mathrm{s}^{-1}$  determined by the uncertainty in the instrumental zero  $(1.5 \, \text{s}^{-1})$  of the OH reactivity instrument. This uncertainty was applied in sensitivity runs of the model, but had a minor effect on the results discussed here.

The unknown chemical nature of the background reactivity that dominates the loss of OH radicals for the zero-air phase of the experiment strongly limits the ability of the simple model used during this phase in reproducing the measured radical concentrations. Additional parameters such as, for example, a loss path for HO<sub>2</sub> radicals could improve the agreement with the model results but would hinder the concept of using a simple model. A test run of the model using CH<sub>4</sub> as species Y instead of CO was performed and the results are shown in Fig. S1 of the Supplement. It can be clearly seen that using CH<sub>4</sub> as species Y instead of CO does increase the agreement between measured and modelled HO<sub>2</sub> radicals during the zero-air phase, but has a negligible impact on the agreement observed once the MBO is injected. This underlines how the radical concentrations are insensitive to the nature of the Y species once the MBO is present in the chamber. As the zero-air phase serves to check the status of the chamber to identify, for example, unexpected contamination and has no impact on the chemistry once MBO dominates the OH reactivity, no model calculation is shown for this part of the experiment in the following.

Because of the unknown chemical nature of the background reactivity that dominates the loss of OH radicals for the zero-air phase of the experiment, agreement between measured and modelled radical concentrations cannot be expected during this initial phase. Therefore, no model calculation is shown for this part of the experiment.

Photolysis frequencies (*j* values) for O<sub>3</sub>, NO<sub>2</sub>, HONO, hydrogen peroxide (H2O2), and formaldehyde were constrained to the measurements. All the other photolysis frequencies present in the model were first calculated for clear sky conditions according to the MCM 3.3.1 and then scaled by the ratio of measured to calculated  $j(NO_2)$  to account for clouds and transmission of the chamber film. The model was constrained to measured water vapour, chamber pressure (ambient pressure), and temperature, as well as NO, NO<sub>2</sub>, and HONO. Values were reinitiated every minute. MBO and O<sub>3</sub> injections were implemented in the model by applying a source just active for the time of the injection. The O<sub>3</sub> source was adjusted to match the concentration measured at the injection and the MBO source to match the change in OH reactivity at the injection time. For completeness, the model included the reaction of MBO with O<sub>3</sub> although this reaction contributed on average 3 % to the reactivity of MBO which was dominated by the reaction with OH radicals.

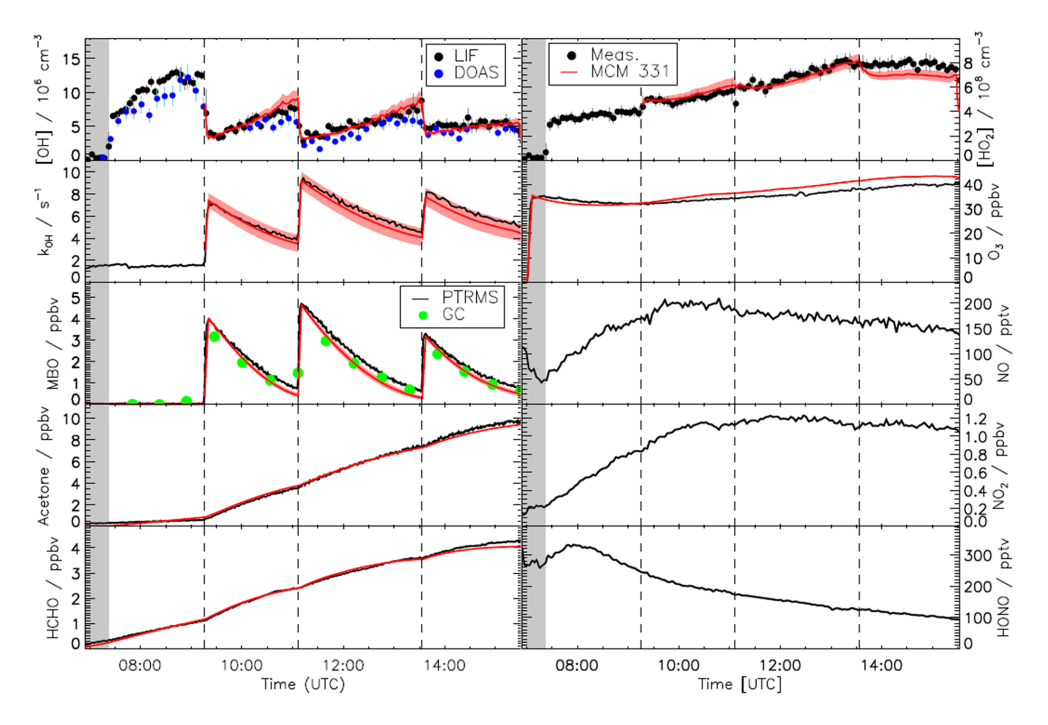


**Figure 2.** Measured time series of OH, HO<sub>2</sub>, MBO, acetone, formaldehyde, O<sub>3</sub>, trace gases, and OH reactivity compared to results obtained from modelling using the MCM version 3.3.1. There are no model results for NO, NO<sub>2</sub>, or HONO as the model was constrained to the measurements. The red shaded areas represent the uncertainty in the model due to the uncertainties of the zero of the OH reactivity measurements (see text for details). Grey shaded areas indicate the times before opening the chamber roof and vertical dashed lines indicate the times when MBO was injected.

#### 3 Results and discussion

# 3.1 Model comparison

Figure 2 shows the time series for the trace gases measured during the MBO experiment compared to the model including the sensitivity runs for the uncertainty introduced by the zero OH-reactivity value. At the beginning of the experiment, during the dark phase, formation of radicals was not expected as the roof was closed and only water vapour and ozone were added. The reactivity of 1.7 s<sup>-1</sup> observed during this phase was due to desorption of trace gases from the walls of the chamber that could be observed during the humidification process. Some of these trace gases are HONO, HCHO, and acetone as seen from their slow but steady increase. Immediately after opening of the roof, there was production of OH and HO<sub>2</sub> radicals and NO<sub>x</sub> from the photolysis of HONO and HCHO. After the injection of MBO, the OH reactivity was dominated by the reaction with MBO ( $\sim 70\%$  for all three MBO injections) and its oxidation products contributed significantly to the OH reactivity, up to 40 %, once most of the MBO had reacted away. Good agreement between modelled and measured concentrations, well within the accuracy of the different instruments, could be observed for the majority of the species when MBO was oxidized by OH in this experiment. Formation of both measured major products from the oxidation of MBO, formaldehyde, and acetone was well reproduced by the model (averaged measurement to model ratio of  $1.00\pm0.02$  for both). The modelled OH fitted the observation with an average measurement to model ratio of  $1.0\pm0.2$  and the agreement between modelled and measured HO<sub>2</sub>, although less good compared to the OH, was still satisfying  $(0.9\pm0.1)$ . The MBO decays due to its reaction with OH radicals were slightly overpredicted by the model (average observed to model ratio of  $1.3\pm0.2$ ) in accordance with the measured decline of OH reactivity. This is in agreement with the PTR-TOF-MS measurement. However, results did not change significantly if the model was constrained to measured MBO concentrations.

The major uncertainties in this measurement–model comparison are introduced by the uncertainty of the zero measurement of the OH reactivity data and by the possible interference of RO<sub>2</sub> radicals in the measured HO<sub>2</sub> signal. The first mostly affects the agreement between measured and modelled results for the OH reactivity itself. Modelled OH and HO<sub>2</sub> radicals are also partially affected but the uncertainty introduced is lower than the accuracy of radical measurements while the remaining modelled species are not influenced. As mentioned in the instrumental description section, 20 % is the upper limit for the interference from RO<sub>2</sub> radicals that could be expected from MBO on the HO<sub>2</sub> signal, based on the experiments performed with isoprene (Fuchs et al., 2011) for the conditions the instrument was run with. The

 $\rm HO_2$  concentration obtained from the model when accounting for this  $\rm RO_2$  interference would be, on average, only 8 % larger ( $\sim 5.5 \times 10^7 \, \rm cm^{-3}$ ) than the  $\rm HO_2$  concentration without any  $\rm RO_2$  interference for the periods in the experiment where the MBO was present in the chamber. This value is lower than the accuracy of the  $\rm HO_2$  measurement itself and has an insignificant impact on the other trace gases.

# 3.2 Model comparison including hydrogen shift reactions

In a recent theoretical work from Knap et al. (2016), hydrogen shift reactions (H-shift) in the peroxy radicals originated after photooxidation of four different methyl-buten-ol isomers were investigated. The 1,4, 1,5 and 1,6 H-shift reactions were studied and the rate coefficients at ambient temperature and pressure were given. For the photooxidation of the MBO isomer under investigation in this study, predicted products are OH and HO<sub>2</sub> radicals, 2-hydroxy-2-methylpropanal (HMPR), acetone, and glycolaldehyde (Fig. 1). Also  $\beta$ and  $\delta$ -epoxides are proposed as possible products although, due to their extremely slow unimolecular rate coefficients (Fig. 1), they are insignificant. As a sensitivity study, the three H-shift reactions, excluding the branching towards the epoxides, were included in the MCM 3.3.1 model as shown in Fig. 1, using the upper limit rate coefficients at 1013 hPa and 298 K as calculated by Knap et al. (2016). In the model, the H-shift reactions proceed directly to the final stable products without formation of intermediates. As expected from the low reaction rates for these reactions, their addition to the MBO degradation scheme has a very small impact with a change of less than 1% on any of the trace gases modelled in our chamber study bringing no improvement in the already good agreement between measurements and model calculations. This is consistent with the study by Knap et al. (2016) where they concluded that H-shift reactions are not relevant for the oxidation scheme of MBO even for low NO conditions (< 50 pptv), where the reaction with HO<sub>2</sub> remains the dominant loss process for the MBO-RO<sub>2</sub> radicals. This is also expected as MBO contains only one double bond and the fast H-shift reactions observed for isoprene and methacrolein are favoured by the formation of conjugated double bonds in the stable radical co-products (Peeters and Nguyen, 2012).

# 3.3 OH and HO<sub>2</sub> radicals budget analysis

The calculation of the experimental OH budget helps with identifying possible missing OH sources, assuming the correctness of the measured OH concentration and OH reactivity. The total experimental OH loss rate,  $L_{\rm OH}$ , is given by the product of the OH concentration and the OH reactivity and, as the OH radical is assumed to be in steady-state, it should be equal to the total OH production rate ( $P_{\rm OH}$ ; Eq. 1);  $P_{\rm OH}$  includes the OH production rate from known sources,  $P_{\rm OH}$ Meas (Eq. 2), plus other possible sources;  $L_{\rm OH}$  can be

compared with  $P_{\text{OH}}$ Meas, which can be calculated from the measured data.

$$L_{\text{OH}} = k_{\text{OH}} \times [\text{OH}] \approx P_{\text{OH}} = P_{\text{OH}} \text{Meas} + \text{other sources} \quad (1)$$

$$P_{\text{OH}} \text{Meas} = ([\text{HO}_2] \times [\text{NO}] \times k_{\text{HO}_2 + \text{NO}})$$

$$+ ([\text{HONO}] \times j(\text{HONO})) + ([\text{O}_3] \times j(\text{O}^1 \text{D}) \times y)$$

$$+ ([\text{HO}_2] \times [\text{O}_3] \times k_{\text{HO}_2 + \text{O}_3}) \quad (2)$$

Here [OH], [HO<sub>2</sub>], [NO], [HONO], and [O<sub>3</sub>] represent the measured concentrations of the trace gases;  $k_{\text{HO}_2+\text{NO}}$  and  $k_{\text{HO}_2+\text{O}_3}$  the rate coefficients of HO<sub>2</sub> with NO and ozone, respectively; j (HONO) and j (O<sup>1</sup>D) the photolysis rates of HONO and O<sub>3</sub>, respectively; and y is the fraction of O(<sup>1</sup>D) reacting with water vapour multiplied with the OH yield of the O(<sup>1</sup>D) + H<sub>2</sub>O reaction. If all the sources contributing to the OH production are included in the calculation, then  $P_{\text{OH}}$ Meas  $\approx P_{\text{OH}}$ . In this study, the known OH sources considered are the following: reaction of NO and HO<sub>2</sub>, reaction of O<sub>3</sub> and HO<sub>2</sub>, photolysis of HONO, and photolysis of O<sub>3</sub>. The formation of OH from ozonolysis of MBO is not included as it does not contribute noticeably.

Figure 3 shows the comparison between  $P_{\rm OH}$ Meas and the total experimental OH loss,  $L_{\rm OH}$ . The averaged ratio between  $P_{\rm OH}$ Meas and  $L_{\rm OH}$  is  $0.9\pm0.1~(1\sigma)$ . A small deviation from unity, which would indicate a missing OH source contributing at most 20% to the total OH production, is obtained. Nevertheless, if the errors of the different measurements are taken into account, this deviation becomes insignificant. For example, the total error of the total experimental OH loss is  $\sim 17\%$  to which the errors of the measured traces gases, mainly of the HO<sub>2</sub> radicals (16%) and of the rate coefficients ( $\sim 10\%$ ) used to calculate the  $P_{\rm OH}$ Meas, should be added. From these considerations, the experimental OH budget can be considered closed and no additional OH sources aside from the ones considered in Eq. (2) are needed to explain the OH radicals loss.

Figure 3 also depicts the total modelled OH production P<sub>OH</sub>Mod. This is included in the analysis of the experimental OH radical budget to understand how well the OHformation paths in the model can describe the measurements. The averaged ratio between  $P_{OH}Mod$  and  $L_{OH}$  provides a value of  $1.0 \pm 0.1$  (1 $\sigma$ ). The good agreement observed between  $P_{\text{OH}}\text{Mod}$  and  $L_{\text{OH}}$  indicates that the model is able to correctly represent the OH radical sources. The averaged difference between  $P_{\rm OH}{
m Mod}$  and  $P_{\rm OH}{
m Meas}$  is (2.3  $\pm$ 1.9)  $\times$   $10^6$  cm<sup>-3</sup> s<sup>-1</sup>. A large part of the difference,  $\sim$   $1.5 \times$ 10<sup>6</sup> cm<sup>-3</sup> s<sup>-1</sup>, is due to additional OH radical sources included in the model and not considered in the experimental OH production, e.g. RO<sub>2</sub> (CH<sub>3</sub>CO<sub>3</sub> and HOCH<sub>2</sub>CO<sub>3</sub>) reacting with HO2 forming OH. The additional small discrepancy  $(\sim 0.8 \times 10^6 \, \text{cm}^{-3} \, \text{s}^{-1})$  is due to the differences observed for HO<sub>2</sub> and ozone between measurements and model calculations.

The analysis of the HO<sub>2</sub> budget is shown in Fig. 4. Here, different from the OH budget, the measured HO<sub>2</sub> loss rate,

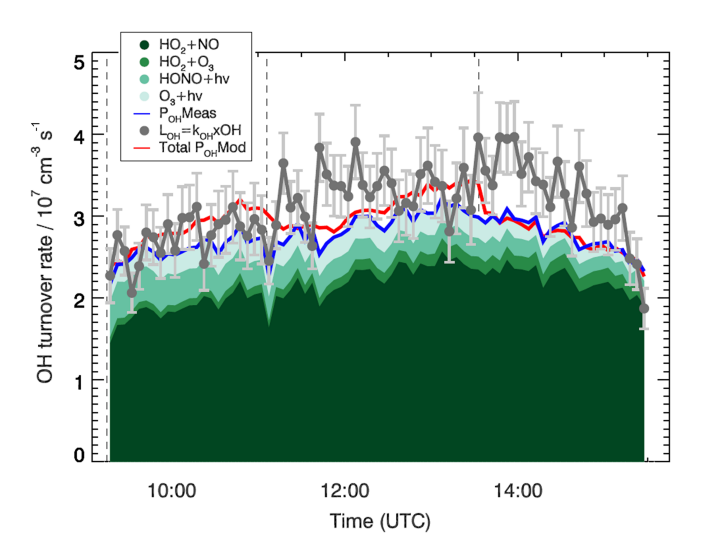


**Figure 3.** OH budget for the MBO experiment. The experimentally determined total OH loss rate,  $L_{\rm OH}$ , and individual production terms are shown. For comparison, the red line indicates the total modelled OH production,  $P_{\rm OH}$ Mod, which equals the modelled loss rate. Vertical dashed lines indicate the times when MBO was injected. Error bars  $(1\sigma)$  for  $L_{\rm OH}$  include the accuracy of measurements.

 $L_{\rm HO_2}$ , is compared to the total modelled HO<sub>2</sub> production rate, P<sub>HO2</sub>Mod. This comparison provides information on the completeness in the understanding of the HO<sub>2</sub> production and loss processes for the MBO photooxidation mechanism. Within the model, the 15 most important HO<sub>2</sub> production paths are explicitly considered and depicted in Fig. 4. The largest contribution to the HO<sub>2</sub> production comes from decomposition of alkoxy radicals with a subsequent reaction with oxygen (51%, see, as an example, reaction of MBOAO from Fig. 1), followed by the conversion of OH by species Y (20%) which is specific to the SAPHIR chamber and therefore not atmospherically relevant. Smaller contributions originate from formaldehyde photolysis (18%), and H-abstraction reaction by oxygen from the methoxy radical (CH<sub>3</sub>O, 8%). As most of the relevant species contributing to the HO<sub>2</sub> production rate such as the alkoxy radicals were not measured and the background reactivity Y cannot be specified, it is not possible to calculate the production rate of HO<sub>2</sub> only from measured species as it was done for the OH radical budget.

The  $HO_2$  radical is expected to be lost mainly via its reaction with NO accounting for  $\sim 90\,\%$  of the total loss rate calculated from the model. Additional losses are  $HO_2+HO_2$  self-reaction, reaction with ozone, and reaction with the first generation  $RO_2$  produced from the MBO oxidation (MBOAO2 and MBOBO2, Fig. 1). Therefore, the majority of the  $HO_2$  loss rate can be obtained from measured NO,  $HO_2$ , and ozone concentrations (Eq. 3).

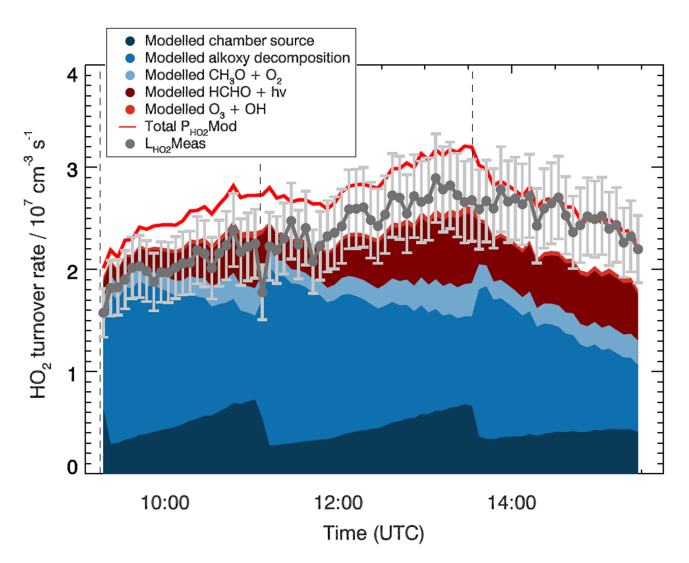


**Figure 4.** HO<sub>2</sub> budget for the MBO experiment. The loss rate of HO<sub>2</sub> calculated from measured NO, ozone, and HO<sub>2</sub> concentrations,  $L_{\rm HO_2}$ Meas, and individual modelled production terms are shown. For comparison, the red line indicates the total modelled HO<sub>2</sub> production,  $P_{\rm HO_2}$ Mod, which equals the total modelled loss rate. Vertical dashed lines indicate the times when MBO was injected. Error bars (1 $\sigma$ ) for  $L_{\rm HO_2}$ Meas include the accuracy of HO<sub>2</sub> measurements.

$$L_{\text{HO}_2}\text{Meas} = ([\text{HO}_2] \times [\text{NO}] \times k_{\text{HO}_2+\text{NO}}) + ([\text{HO}_2] \times [\text{HO}_2] \times k_{\text{HO}_2+\text{HO}_2}) + ([\text{HO}_2] \times [\text{O}_3] \times k_{\text{HO}_2+\text{O}_3})$$
(3)

Here [HO<sub>2</sub>], [NO], and [O<sub>3</sub>] represent the measured concentrations of the trace gases,  $k_{\text{HO}_2+\text{NO}}$ ,  $k_{\text{HO}_2+\text{HO}_2}$ , and  $k_{\text{HO}_2+\text{O}_3}$ the rate coefficients of HO<sub>2</sub> with NO, itself, and O<sub>3</sub>, respectively. The measured  $HO_2$  loss rate,  $L_{HO_2}Meas$ , is in good agreement with the total modelled HO<sub>2</sub> production rate with an average ratio of measured to modelled rates of  $0.8 \pm 0.1$ . The agreement with the total modelled  $HO_2$ production increases (average ratio of measured to modelled rates of  $0.9\pm0.1$ ) when including in the  $L_{\text{HO}_2}$  Meas the modelled loss rate by the reaction of HO2 with modelled RO2 radicals. The largest discrepancies are observed during the first injection of MBO, because the calculated HO<sub>2</sub> production rate is smaller than what is obtained from the model. The main reason is the lower measured HO<sub>2</sub> concentration (13%) compared to the model during this period. With the increasing agreement between modelled and measured HO<sub>2</sub> radical also the agreement in the HO<sub>2</sub> budget increases.

The good agreement observed in the  $HO_2$  budget, although partly relying on modelled species concentrations, indicates that the  $HO_2$  production, within this chamber experiment, can be explained by alkoxy radical decomposition, photolysis of formaldehyde, and the chamber-specific Y source.

# 3.4 Comparison with previous studies

MBO was the major BVOC measured in two field campaigns which included measurements of OH and HO<sub>2</sub> radicals and a comparison with model calculations. The Biosphere Effects on Aerosols and Photochemisty Experiment II (BEARPEX09) campaign was performed near the Blodgett Forest Research Station in the Californian Sierra Nevada mountains (Mao et al., 2012). This campaign was characterized by large MBO concentrations (daily average  $\sim 3000$  pptv), followed by isoprene (daily average  $\sim 1700$  pptv) and monoterpenes (\$\alpha\$-pinene, daily average 100 pptv and \$\beta\$-pinene, daily average 70 pptv). Both measured OH and HO<sub>2</sub> radicals compared reasonably well with modelled calculations, in agreement with the results observed in this chamber study.

The 2010 Bio-hydro-atmosphere interactions of Energy, Aerosols, Carbon, H<sub>2</sub>O, Organics and Nitrogen - Rocky Mountain Organic Carbon Study (BEACHON-ROCS) was performed in the Manitou Experimental Forest in the Front Range of the Rocky Mountains in Colorado (Ortega et al., 2014). Here the dominantly measured BVOC was MBO (daily average ~ 1600 pptv) followed by monoterpenes (daily average  $\sim 500$  pptv) (Kim et al., 2013). As observed for the OH radical budget within this study, during the BEACHON-ROCS campaign the calculated OH concentration from ozone photolysis and from the recycling via HO<sub>2</sub> plus NO reaction, divided by the measured OH reactivity, agreed with the measured OH concentration (Kim et al., 2013). No additional OH recycling paths were necessary to close the OH budget. Nevertheless, during the BEACHON-ROCS campaign, the model was able to reproduce the OH radical concentration only when constrained to the HO<sub>2</sub> radical measurements as the model underestimated the measured HO<sub>2</sub> radicals up to a factor of 3 (Kim et al., 2013; Wolfe et al., 2014). This is different from what was observed in the chamber experiment discussed in this study where a good agreement was found between modelled and measured HO<sub>2</sub> concentration. The base models used during both campaigns contained the same MBO oxidation scheme as tested in this study and as described in the MCM 3.3.1.

One difference between the two field studies is the BVOC compositions. During the BEARPEX09 campaign, the concentration of the measured monoterpenes relative to the concentration of MBO during daytime was smaller (6%) compared to what was observed during the BEACHONROCS campaign (31%). Two recent studies in environments with large concentrations of monoterpenes (Hens et al., 2014; Kaminski et al., 2017) also showed model calculations largely underestimating HO<sub>2</sub> radical measurements. Both studies concluded that the unaccounted HO<sub>2</sub> source seems to originate from monoterpene-oxidation products. The results collected by Hens et al. (2014) and by Kaminski et al. (2017) together with what is observed in this chamber study support that model–measurement discrepancies for

HO<sub>2</sub> radicals in the BEACHON-ROCS campaign are not related to the MBO and its oxidation products but rather to the presence of monoterpenes and, as they were present in smaller concentrations, they would need to constitute a very efficient source of HO<sub>2</sub> radicals.

# 4 Summary and conclusions

A photooxidation experiment on 2-methyl-3-butene-2-ol (MBO), an important BVOC emitted by lodgepole and ponderosa pines, was performed in the atmospheric simulation chamber SAPHIR. Measurements of OH and HO2 radicals and OH reactivity together with other important trace gases were compared to results from a state-of-the-art chemical mechanistic model (MCM v3.3.1). The overall agreement is very good: firstly, an average observed to modelled ratio of  $1.0\pm0.2$  and  $0.9\pm0.1$  is found for OH and HO<sub>2</sub> radicals, respectively. Also the MBO decay caused by reaction with OH radicals fits the expected decay from the model (average observed to modelled ratio of MBO concentration of  $1.3 \pm 0.2$ ) and is consistent with the measured OH reactivity. Moreover, the major measured products, acetone, and formaldehyde, both match the model calculation with an average ratio of  $1.00 \pm 0.02$ . Addition of H-shift reactions from RO<sub>2</sub> radicals to the kinetic model as suggested in the literature (Knap et al., 2016) does not have a significant impact on the model results as expected from the small reaction rates ( $< 1.1 \times 10^{-3} \text{ s}^{-1}$ ). The observed closure for both OH and HO2 radical budgets indicates that their chemistry is well described by our current understanding of the MBO OH-initiated degradation

The good agreement within the experimental OH budget is consistent with what was observed in previous field campaigns where MBO was the dominant BVOC measured (Mao et al., 2012; Kim et al., 2013). However, there was no closure for the HO<sub>2</sub> budget or agreement between measurements and model results when a larger concentration of monoterpenes was also observed (Wolfe et al., 2014). This discrepancy cannot be explained by MBO photooxidation as a good agreement between measured and calculated concentration of HO<sub>2</sub> is found in this chamber study. As large discrepancies were also observed for chamber studies with  $\beta$ -pinene (Kaminski et al., 2017) and in environments with large monoterpene concentrations (Hens et al., 2014), it is reasonable to assume that field observation for HO<sub>2</sub> radicals could be explained by an additional HO<sub>2</sub> radical source from monoterpene oxidation products, as proposed by Kaminski et al. (2017).

Data availability. The data from the experiment in the SAPHIR chamber used in this work are available on the EUROCHAMP data homepage (https://data.eurochamp.org/, last access: August 2018).

The Supplement related to this article is available online at https://doi.org/10.5194/acp-18-11409-2018-supplement.

Author contributions. HF and AH designed the experiments. HF conducted the  $HO_x$  radical measurements and SN was responsible for the OH reactivity measurements. BB conducted the radiation measurements. MK and RW were responsible for the GC measurements. RT, AL, and IHA were responsible for the PTR-MS measurements. XL was responsible for the HONO measurements and HPD for the DOAS OH data. FR was responsible for the  $NO_x$  and  $NO_x$  an

Competing interests. The authors declare that they have no conflict of interest.

Acknowledgements. This work was supported by the EU FP-7 program EUROCHAMP-2 (grant agreement no. 228335). This project has received funding from the European Research Council (ERC) under the European Union's Horizon 2020 research and innovation program (SARLEP grant agreement no. 681529).

The article processing charges for this open-access publication were covered by a Research Centre of the Helmholtz Association.

Edited by: Dwayne Heard

Reviewed by: two anonymous referees

# References

- Bohn, B. and Zilken, H.: Model-aided radiometric determination of photolysis frequencies in a sunlit atmosphere simulation chamber, Atmos. Chem. Phys., 5, 191–206, https://doi.org/10.5194/acp-5-191-2005, 2005.
- Bohn, B., Rohrer, F., Brauers, T., and Wahner, A.: Actinometric measurements of NO<sub>2</sub> photolysis frequencies in the atmosphere simulation chamber SAPHIR, Atmos. Chem. Phys., 5, 493–503, https://doi.org/10.5194/acp-5-493-2005, 2005.
- Carrasco, N., Doussin, J. F., Picquet-Varrault, B., and Carlier, P.: Tropospheric degradation of 2-hydroxy-2-methylpropanal, a photo-oxidation product of 2-methyl-3-buten-2-ol: Kinetic and mechanistic study of its photolysis and its reaction with OH radicals, Atmos. Environ., 40, 2011–2019, https://doi.org/10.1016/j.atmosenv.2005.11.042, 2006.
- Carslaw, N., Creasey, D. J., Harrison, D., Heard, D. E., Hunter, M. C., Jacobs, P. J., Jenkin, M. E., Lee, J. D., Lewis, A. C., Pilling, M. J., Saunders, S. M., and Seakins, P. W.: OH and HO<sub>2</sub> radical chemistry in a forested region of north-western Greece, Atmos. Environ. , 35, 4725–4737, https://doi.org/10.1016/S1352-2310(01)00089-9, 2001.

- Crounse, J. D., Paulot, F., Kjaergaard, H. G., and Wennberg, P. O.: Peroxy radical isomerization in the oxidation of isoprene, Phys. Chem. Chem. Phys., 13, 13607–13613, https://doi.org/10.1039/c1cp21330j, 2011.
- Crounse, J. D., Knap, H. C., Ørnsø, K. B., Jørgensen, S., Paulot, F., Kjaergaard, H. G., and Wennberg, P. O.: Atmospheric Fate of Methacrolein. 1. Peroxy Radical Isomerization Following Addition of OH and O<sub>2</sub>, J. Phys. Chem. A, 116, 5756–5762, https://doi.org/10.1021/jp211560u, 2012.
- D'Ambro, E. L., Møller, K. H., Lopez-Hilfiker, F. D., Schobesberger, S., Liu, J., Shilling, J. E., Lee, B. H., Kjaergaard, H. G., and Thornton, J. A.: Isomerization of Second-Generation Isoprene Peroxy Radicals: Epoxide Formation and Implications for Secondary Organic Aerosol Yields, Environ. Sci. Technol., 51, 4978–4987, https://doi.org/10.1021/acs.est.7b00460, 2017.
- da Silva, G.: Hydroxyl radical regeneration in the photochemical oxidation of glyoxal: kinetics and mechanism of the HC(O)CO + O<sub>2</sub> reaction, Phys. Chem. Chem. Phys., 12, 6698–6705, https://doi.org/10.1039/b927176g, 2010.
- da Silva, G.: Reaction of Methacrolein with the Hydroxyl Radical in Air: Incorporation of Secondary O<sub>2</sub> Addition into the MACR + OH Master Equation, J. Phys. Chem. A, 116, 5317–5324, https://doi.org/10.1021/jp303806w, 2012.
- Dibble, T. S.: Intramolecular Hydrogen Bonding and Double H-Atom Transfer in Peroxy and Alkoxy Radicals from Isoprene, J. Phys. Chem. A, 108, 2199–2207, https://doi.org/10.1021/jp0306702, 2004.
- Dillon, T. J. and Crowley, J. N.: Direct detection of OH formation in the reactions of HO<sub>2</sub> with CH<sub>3</sub>C(O)O<sub>2</sub> and other substituted peroxy radicals, Atmos. Chem. Phys., 8, 4877–4889, https://doi.org/10.5194/acp-8-4877-2008, 2008.
- Dorn, H.-P., Brandenburger, U., Brauers, T., and Hausmann, M.: A New In Situ Laser Long-Path Absorption Instrument for the Measurement of Tropospheric OH Radicals, J. Atmos. Sci., 52, 3373–3380, https://doi.org/10.1175/1520-0469(1995)052<3373:anisll>2.0.co;2, 1995.
- Fantechi, G., Jensen, N. R., Hjorth, J., and Peeters, J.: Mechanistic studies of the atmospheric oxidation of methyl butenol by OH radicals, ozone and NO<sub>3</sub> radicals, Atmos. Environ., 32, 3547–3556, https://doi.org/10.1016/S1352-2310(98)00061-2, 1998.
- Feierabend, K. J., Zhu, L., Talukdar, R. K., and Burkholder, J. B.: Rate Coefficients for the OH+HC(O)C(O)H (Glyoxal) Reaction between 210 and 390 K, J. Phys. Chem. A, 112, 73–82, https://doi.org/10.1021/jp0768571, 2008.
- Ferronato, C., Orlando, J. J., and Tyndall, G. S.: Rate and mechanism of the reactions of OH and Cl with 2-methyl-3-buten-2-ol, Nat. Geosci., 103, 25579–25586, https://doi.org/10.1029/98JD00528, 1998.
- Fuchs, H., Bohn, B., Hofzumahaus, A., Holland, F., Lu, K. D., Nehr, S., Rohrer, F., and Wahner, A.: Detection of  $\rm HO_2$  by laser-induced fluorescence: calibration and interferences from  $\rm RO_2$  radicals, Atmos. Meas. Tech., 4, 1209–1225, https://doi.org/10.5194/amt-4-1209-2011, 2011.
- Fuchs, H., Dorn, H.-P., Bachner, M., Bohn, B., Brauers, T., Gomm,
  S., Hofzumahaus, A., Holland, F., Nehr, S., Rohrer, F., Tillmann,
  R., and Wahner, A.: Comparison of OH concentration measurements by DOAS and LIF during SAPHIR chamber experiments
  at high OH reactivity and low NO concentration, Atmos. Meas.

- Tech., 5, 1611–1626, https://doi.org/10.5194/amt-5-1611-2012, 2012
- Fuchs, H., Hofzumahaus, A., Rohrer, F., Bohn, B., Brauers, T., Dorn, H. P., Haseler, R., Holland, F., Kaminski, M., Li, X., Lu, K., Nehr, S., Tillmann, R., Wegener, R., and Wahner, A.: Experimental evidence for efficient hydroxyl radical regeneration in isoprene oxidation, Nat. Geosci., 6, 1023–1026, https://doi.org/10.1038/Ngeo1964, 2013.
- Fuchs, H., Acir, I.-H., Bohn, B., Brauers, T., Dorn, H.-P., Häseler, R., Hofzumahaus, A., Holland, F., Kaminski, M., Li, X., Lu, K., Lutz, A., Nehr, S., Rohrer, F., Tillmann, R., Wegener, R., and Wahner, A.: OH regeneration from methacrolein oxidation investigated in the atmosphere simulation chamber SAPHIR, Atmos. Chem. Phys., 14, 7895–7908, https://doi.org/10.5194/acp-14-7895-2014, 2014.
- Fuchs, H., Tan, Z., Hofzumahaus, A., Broch, S., Dorn, H.-P., Holland, F., Künstler, C., Gomm, S., Rohrer, F., Schrade, S., Tillmann, R., and Wahner, A.: Investigation of potential interferences in the detection of atmospheric RO<sub>x</sub> radicals by laser-induced fluorescence under dark conditions, Atmos. Meas. Tech., 9, 1431–1447, https://doi.org/10.5194/amt-9-1431-2016, 2016.
- Fuchs, H., Novelli, A., Rolletter, M., Hofzumahaus, A., Pfannerstill,
  E. Y., Kessel, S., Edtbauer, A., Williams, J., Michoud, V., Dusanter, S., Locoge, N., Zannoni, N., Gros, V., Truong, F., Sarda-Esteve, R., Cryer, D. R., Brumby, C. A., Whalley, L. K., Stone, D., Seakins, P. W., Heard, D. E., Schoemaecker, C., Blocquet, M., Coudert, S., Batut, S., Fittschen, C., Thames, A. B., Brune, W. H., Ernest, C., Harder, H., Muller, J. B. A., Elste, T., Kubistin, D., Andres, S., Bohn, B., Hohaus, T., Holland, F., Li, X., Rohrer, F., Kiendler-Scharr, A., Tillmann, R., Wegener, R., Yu, Z., Zou, Q., and Wahner, A.: Comparison of OH reactivity measurements in the atmospheric simulation chamber SAPHIR, Atmos. Meas. Tech., 10, 4023–4053, https://doi.org/10.5194/amt-10-4023-2017, 2017.
- Goldan, P. D., Kuster, W. C., Fehsenfeld, F. C., and Montzka, S. A.: The observation of a C<sub>5</sub> alcohol emission in a North American pine forest, Geophys. Res. Lett., 20, 1039–1042, https://doi.org/10.1029/93GL00247, 1993.
- Griffith, S. M., Hansen, R. F., Dusanter, S., Stevens, P. S., Alaghmand, M., Bertman, S. B., Carroll, M. A., Erickson, M., Galloway, M., Grossberg, N., Hottle, J., Hou, J., Jobson, B. T., Kammrath, A., Keutsch, F. N., Lefer, B. L., Mielke, L. H., O'Brien, A., Shepson, P. B., Thurlow, M., Wallace, W., Zhang, N., and Zhou, X. L.: OH and HO<sub>2</sub> radical chemistry during PROPHET 2008 and CABINEX 2009 Part 1: Measurements and model comparison, Atmos. Chem. Phys., 13, 5403–5423, https://doi.org/10.5194/acp-13-5403-2013, 2013.
- Groß, C. B. M., Dillon, T. J., Schuster, G., Lelieveld, J., and Crowley, J. N.: Direct Kinetic Study of OH and O<sub>3</sub> Formation in the Reaction of CH<sub>3</sub>C(O)O<sub>2</sub> with HO<sub>2</sub>, J. Phys. Chem. A, 118, 974–985, https://doi.org/10.1021/jp412380z, 2014.
- Guenther, A. B., Jiang, X., Heald, C. L., Sakulyanontvittaya, T., Duhl, T., Emmons, L. K., and Wang, X.: The Model of Emissions of Gases and Aerosols from Nature version 2.1 (MEGAN2.1): an extended and updated framework for modeling biogenic emissions, Geosci. Model Dev., 5, 1471–1492, https://doi.org/10.5194/gmd-5-1471-2012, 2012.

- Harley, P., Fridd-Stroud, V., Greenberg, J., Guenther, A., and Vasconcellos, P.: Emission of 2-methyl-3-buten-2-ol by pines:
  A potentially large natural source of reactive carbon to the atmosphere, J. Geophys. Res.-Atmos., 103, 25479–25486, https://doi.org/10.1029/98JD00820, 1998.
- Hens, K., Novelli, A., Martinez, M., Auld, J., Axinte, R., Bohn, B., Fischer, H., Keronen, P., Kubistin, D., Nölscher, A. C., Oswald, R., Paasonen, P., Petäjä, T., Regelin, E., Sander, R., Sinha, V., Sipilä, M., Taraborrelli, D., Tatum Ernest, C., Williams, J., Lelieveld, J., and Harder, H.: Observation and modelling of HO<sub>x</sub> radicals in a boreal forest, Atmos. Chem. Phys., 14, 8723–8747, https://doi.org/10.5194/acp-14-8723-2014, 2014.
- Hofzumahaus, A., Rohrer, F., Lu, K., Bohn, B., Brauers, T., Chang, C.-C., Fuchs, H., Holland, F., Kita, K., Kondo, Y., Li, X., Lou, S., Shao, M., Zeng, L., Wahner, A., and Zhang, Y.: Amplified Trace Gas Removal in the Troposphere, Science, 324, 1702–1704, https://doi.org/10.1126/science.1164566, 2009.
- Holland, F., Hofzumahaus, A., Schafer, R., Kraus, A., and Patz, H. W.: Measurements of OH and HO(2) radical concentrations and photolysis frequencies during BERLIOZ, J. Geophys. Res.-Atmos., 108, PHO 2-1-PHO 2-23, https://doi.org/10.1029/2001jd001393, 2003.
- Hornbrook, R. S., Crawford, J. H., Edwards, G. D., Goyea, O., Mauldin III, R. L., Olson, J. S., and Cantrell, C. A.: Measurements of tropospheric HO<sub>2</sub> and RO<sub>2</sub> by oxygen dilution modulation and chemical ionization mass spectrometry, Atmos. Meas. Tech., 4, 735–756, https://doi.org/10.5194/amt-4-735-2011, 2011.
- Jenkin, M. E., Saunders, S. M., and Pilling, M. J.: The tropospheric degradation of volatile organic compounds: A protocol for mechanism development, Atmos. Environ., 31, 81–104, https://doi.org/10.1016/S1352-2310(96)00105-7, 1997.
- Jordan, A., Haidacher, S., Hanel, G., Hartungen, E., Mark, L., Seehauser, H., Schottkowsky, R., Sulzer, P., and Mark, T. D.: A high resolution and high sensitivity proton-transfer-reaction time-of-flight mass spectrometer (PTR-TOF-MS), Int. J. Mass. Spectrom., 286, 122–128, https://doi.org/10.1016/j.ijms.2009.07.005, 2009.
- Kaminski, M., Fuchs, H., Acir, I.-H., Bohn, B., Brauers, T., Dorn, H.-P., Häseler, R., Hofzumahaus, A., Li, X., Lutz, A., Nehr, S., Rohrer, F., Tillmann, R., Vereecken, L., Wegener, R., and Wahner, A.: Investigation of the β-pinene photooxidation by OH in the atmosphere simulation chamber SAPHIR, Atmos. Chem. Phys., 17, 6631–6650, https://doi.org/10.5194/acp-17-6631-2017, 2017.
- Karl, M., Dorn, H.-P., Holland, F., Koppmann, R., Poppe, D., Rupp, L., Schaub, A., and Wahner, A.: Product study of the reaction of OH radicals with isoprene in the atmosphere simulation chamber SAPHIR, J. Atmos. Chem., 55, 167–187, https://doi.org/10.1007/s10874-006-9034-x, 2006.
- Kelly, T. J. and Fortune, C. R.: Continuous Monitoring of Gaseous Formaldehyde Using an Improved Fluorescence Approach, Int. J. Environ. An. Ch., 54, 249–263, https://doi.org/10.1080/03067319408034093, 1994.
- Kim, S., Wolfe, G. M., Mauldin, L., Cantrell, C., Guenther, A., Karl,
  T., Turnipseed, A., Greenberg, J., Hall, S. R., Ullmann, K., Apel,
  E., Hornbrook, R., Kajii, Y., Nakashima, Y., Keutsch, F. N., Di-Gangi, J. P., Henry, S. B., Kaser, L., Schnitzhofer, R., Graus,
  M., Hansel, A., Zheng, W., and Flocke, F. F.: Evaluation of HO<sub>X</sub>

- sources and cycling using measurement-constrained model calculations in a 2-methyl-3-butene-2-ol (MBO) and monoterpene (MT) dominated ecosystem, Atmos. Chem. Phys., 13, 2031–2044, https://doi.org/10.5194/acp-13-2031-2013, 2013.
- Knap, H. C., Jorgensen, S., and Kjaergaard, H. G.: Theoretical investigation of the hydrogen shift reactions in peroxy radicals derived from the atmospheric decomposition of 3-methyl-3-buten-1-ol (MBO331), Chem. Phys. Lett., 619, 236–240, https://doi.org/10.1016/j.cplett.2014.11.056, 2015.
- Knap, H. C., Schmidt, J. A., and Jorgensen, S.: Hydrogen shift reactions in four methyl-buten-ol (MBO) peroxy radicals and their impact on the atmosphere, Atmos. Environ., 147, 79–87, https://doi.org/10.1016/j.atmosenv.2016.09.064, 2016.
- Kubistin, D., Harder, H., Martinez, M., Rudolf, M., Sander, R., Bozem, H., Eerdekens, G., Fischer, H., Gurk, C., Klüpfel, T., Königstedt, R., Parchatka, U., Schiller, C. L., Stickler, A., Taraborrelli, D., Williams, J., and Lelieveld, J.: Hydroxyl radicals in the tropical troposphere over the Suriname rainforest: comparison of measurements with the box model MECCA, Atmos. Chem. Phys., 10, 9705–9728, https://doi.org/10.5194/acp-10-9705-2010, 2010.
- Lelieveld, J., Butler, T. M., Crowley, J. N., Dillon, T. J., Fischer, H., Ganzeveld, L., Harder, H., Lawrence, M. G., Martinez, M., Taraborrelli, D., and Williams, J.: Atmospheric oxidation capacity sustained by a tropical forest, Nature, 452, 737–740, https://doi.org/10.1038/nature06870, 2008.
- Lew, M. M., Dusanter, S., and Stevens, P. S.: Measurement of interferences associated with the detection of the hydroperoxy radical in the atmosphere using laser-induced fluorescence, Atmos. Meas. Tech., 11, 95–109, https://doi.org/10.5194/amt-11-95-2018, 2018.
- Li, X., Rohrer, F., Hofzumahaus, A., Brauers, T., Häseler, R., Bohn, B., Broch, S., Fuchs, H., Gomm, S., Holland, F., Jäger, J., Kaiser, J., Keutsch, F. N., Lohse, I., Lu, K., Tillmann, R., Wegener, R., Wolfe, G. M., Mentel, T. F., Kiendler-Scharr, A., and Wahner, A.: Missing Gas-Phase Source of HONO Inferred from Zeppelin Measurements in the Troposphere, Science, 344, 292–296, https://doi.org/10.1126/science.1248999, 2014.
- Lindinger, W., Hansel, A., and Jordan, A.: On-line monitoring of volatile organic compounds at pptv levels by means of proton-transfer-reaction mass spectrometry (PTR-MS) Medical applications, food control and environmental research, Int. J. Mass Spectrom., 173, 191–241, https://doi.org/10.1016/S0168-1176(97)00281-4, 1998.
- Lockhart, J., Blitz, M., Heard, D., Seakins, P., and Shannon, R.: Kinetic Study of the OH + Glyoxal Reaction: Experimental Evidence and Quantification of Direct OH Recycling, J. Phys. Chem. A, 117, 11027–11037, https://doi.org/10.1021/jp4076806, 2013.
- Lou, S., Holland, F., Rohrer, F., Lu, K., Bohn, B., Brauers, T.,
  Chang, C. C., Fuchs, H., Häseler, R., Kita, K., Kondo, Y.,
  Li, X., Shao, M., Zeng, L., Wahner, A., Zhang, Y., Wang,
  W., and Hofzumahaus, A.: Atmospheric OH reactivities in
  the Pearl River Delta China in summer 2006: measurement
  and model results, Atmos. Chem. Phys., 10, 11243–11260,
  https://doi.org/10.5194/acp-10-11243-2010, 2010.
- Lu, K. D., Rohrer, F., Holland, F., Fuchs, H., Bohn, B., Brauers, T., Chang, C. C., Häseler, R., Hu, M., Kita, K., Kondo, Y., Li, X., Lou, S. R., Nehr, S., Shao, M., Zeng, L. M., Wahner, A., Zhang, Y. H., and Hofzumahaus, A.: Observation and modelling of OH

- and HO<sub>2</sub> concentrations in the Pearl River Delta 2006: a missing OH source in a VOC rich atmosphere, Atmos. Chem. Phys., 12, 1541–1569, https://doi.org/10.5194/acp-12-1541-2012, 2012.
- Lu, K. D., Hofzumahaus, A., Holland, F., Bohn, B., Brauers, T., Fuchs, H., Hu, M., Häseler, R., Kita, K., Kondo, Y., Li, X., Lou, S. R., Oebel, A., Shao, M., Zeng, L. M., Wahner, A., Zhu, T., Zhang, Y. H., and Rohrer, F.: Missing OH source in a suburban environment near Beijing: observed and modelled OH and HO<sub>2</sub> concentrations in summer 2006, Atmos. Chem. Phys., 13, 1057–1080, https://doi.org/10.5194/acp-13-1057-2013, 2013.
- Mao, J., Ren, X., Zhang, L., Van Duin, D. M., Cohen, R. C., Park, J.-H., Goldstein, A. H., Paulot, F., Beaver, M. R., Crounse, J. D., Wennberg, P. O., DiGangi, J. P., Henry, S. B., Keutsch, F. N., Park, C., Schade, G. W., Wolfe, G. M., Thornton, J. A., and Brune, W. H.: Insights into hydroxyl measurements and atmospheric oxidation in a California forest, Atmos. Chem. Phys., 12, 8009–8020, https://doi.org/10.5194/acp-12-8009-2012, 2012.
- Nakashima, Y., Kato, S., Greenberg, J., Harley, P., Karl, T., Turnipseed, A., Apel, E., Guenther, A., Smith, J., and Kajii, Y.: Total OH reactivity measurements in ambient air in a southern Rocky mountain ponderosa pine forest during BEACHON-SRM08 summer campaign, Atmos. Environ., 85, 1–8, https://doi.org/10.1016/j.atmosenv.2013.11.042, 2014.
- Nehr, S., Bohn, B., and Wahner, A.: Prompt HO<sub>2</sub> Formation Following the Reaction of OH with Aromatic Compounds under Atmospheric Conditions, J. Phys. Chem. A, 116, 6015–6026, https://doi.org/10.1021/jp210946y, 2011.
- Nguyen, T. L., Vereecken, L., and Peeters, J.:  $HO_x$  Regeneration in the Oxidation of Isoprene III: Theoretical Study of the key Isomerisation of the Z- $\delta$ -hydroxyperoxy Isoprene Radicals, Chem.Phys.Chem., 11, 3996–4001, https://doi.org/10.1002/cphc.201000480, 2010.
- Novelli, A., Hens, K., Tatum Ernest, C., Kubistin, D., Regelin, E., Elste, T., Plass-Dülmer, C., Martinez, M., Lelieveld, J., and Harder, H.: Characterisation of an inlet pre-injector laser-induced fluorescence instrument for the measurement of atmospheric hydroxyl radicals, Atmos. Meas. Tech., 7, 3413–3430, https://doi.org/10.5194/amt-7-3413-2014, 2014.
- Ortega, J., Turnipseed, A., Guenther, A. B., Karl, T. G., Day, D. A., Gochis, D., Huffman, J. A., Prenni, A. J., Levin, E. J. T., Kreidenweis, S. M., DeMott, P. J., Tobo, Y., Patton, E. G., Hodzic, A., Cui, Y. Y., Harley, P. C., Hornbrook, R. S., Apel, E. C., Monson, R. K., Eller, A. S. D., Greenberg, J. P., Barth, M. C., Campuzano-Jost, P., Palm, B. B., Jimenez, J. L., Aiken, A. C., Dubey, M. K., Geron, C., Offenberg, J., Ryan, M. G., Fornwalt, P. J., Pryor, S. C., Keutsch, F. N., DiGangi, J. P., Chan, A. W. H., Goldstein, A. H., Wolfe, G. M., Kim, S., Kaser, L., Schnitzhofer, R., Hansel, A., Cantrell, C. A., Mauldin, R. L., and Smith, J. N.: Overview of the Manitou Experimental Forest Observatory: site description and selected science results from 2008 to 2013, Atmos. Chem. Phys., 14, 6345–6367, https://doi.org/10.5194/acp-14-6345-2014, 2014.
- Peeters, J. and Müller, J.-F.: HO<sub>x</sub> radical regeneration in isoprene oxidation via peroxy radical isomerisations. II: experimental evidence and global impact, Phys. Chem. Chem. Phys, 12, 14227–14235, https://doi.org/10.1039/c0cp00811g, 2010.
- Peeters, J. and Nguyen, T. L.: Unusually Fast 1,6-H Shifts of Enolic Hydrogens in Peroxy Radicals: Formation of the First-Generation C2 and C3 Carbonyls in the Oxi-

- dation of Isoprene, J. Phys. Chem. A, 116, 6134–6141, https://doi.org/10.1021/jp211447q, 2012.
- Peeters, J., Nguyen, T. L., and Vereecken, L.: HO<sub>x</sub> radical regeneration in the oxidation of isoprene, Phys. Chem. Chem. Phys, 11, 5935–5939, https://doi.org/10.1039/b908511d, 2009.
- Peeters, J., Müller, J.-F., Stavrakou, T., and Nguyen, V. S.: Hydroxyl Radical Recycling in Isoprene Oxidation Driven by Hydrogen Bonding and Hydrogen Tunneling: The Upgraded LIM1 Mechanism, J. Phys. Chem. A, 118, 8625–8643, https://doi.org/10.1021/jp5033146, 2014.
- Poppe, D., Brauers, T., Dorn, H.-P., Karl, M., Mentel, T., Schlosser, E., Tillmann, R., Wegener, R., and Wahner, A.: OH-initiated degradation of several hydrocarbons in the atmosphere simulation chamber SAPHIR, J. Atmos. Chem., 57, 203–214, https://doi.org/10.1007/s10874-007-9065-y, 2007.
- Praske, E., Crounse, J. D., Bates, K. H., Kurtén, T., Kjaergaard, H. G., and Wennberg, P. O.: Atmospheric Fate of Methyl Vinyl Ketone: Peroxy Radical Reactions with NO and HO<sub>2</sub>, J. Phys. Chem. A, 119, 4562–4572, https://doi.org/10.1021/jp5107058, 2015.
- Rickly, P. and Stevens, P. S.: Measurements of a potential interference with laser-induced fluorescence measurements of ambient OH from the ozonolysis of biogenic alkenes, Atmos. Meas. Tech., 11, 1–16, https://doi.org/10.5194/amt-11-1-2018, 2018.
- Ridley, B. A., Grahek, F. E., and Walega, J. G.: A Small, High-Sensitivity, Medium-Response Ozone Detector Suitable for Measurements from Light Aircraft, J. Atmos. Ocean. Tech., 9, 142–148, https://doi.org/10.1175/1520-0426(1992)009<0142:ASHSMR>2.0.CO;2, 1992.
- Rohrer, F., Bohn, B., Brauers, T., Brüning, D., Johnen, F.-J., Wahner, A., and Kleffmann, J.: Characterisation of the photolytic HONO-source in the atmosphere simulation chamber SAPHIR, Atmos. Chem. Phys., 5, 2189–2201, https://doi.org/10.5194/acp-5-2189-2005, 2005.
- Rohrer, F., Lu, K., Hofzumahaus, A., Bohn, B., Brauers, T., Chang, C.-C., Fuchs, H., Häseler, R., Holland, F., Hu, M., Kita, K., Kondo, Y., Li, X., Lou, S., Oebel, A., Shao, M., Zeng, L., Zhu, T., Zhang, Y., and Wahner, A.: Maximum efficiency in the hydroxyl-radical-based self-cleansing of the troposphere, Nat. Geosci., 7, 559–563, https://doi.org/10.1038/ngeo2199, 2014.
- Saunders, S. M., Jenkin, M. E., Derwent, R. G., and Pilling, M. J.: Protocol for the development of the Master Chemical Mechanism, MCM v3 (Part A): tropospheric degradation of non-aromatic volatile organic compounds, Atmos. Chem. Phys., 3, 161–180, https://doi.org/10.5194/acp-3-161-2003, 2003.
- Schlosser, E., Bohn, B., Brauers, T., Dorn, H.-P., Fuchs, H., Häseler, R., Hofzumahaus, A., Holland, F., Rohrer, F., Rupp, L., Siese, M., Tillmann, R., and Wahner, A.: Intercomparison of Two Hydroxyl Radical Measurement Techniques at the Atmosphere Simulation Chamber SAPHIR, J. Atmos. Chem., 56, 187–205, https://doi.org/10.1007/s10874-006-9049-3, 2007.
- Schlosser, E., Brauers, T., Dorn, H.-P., Fuchs, H., Häseler, R., Hofzumahaus, A., Holland, F., Wahner, A., Kanaya, Y., Kajii, Y., Miyamoto, K., Nishida, S., Watanabe, K., Yoshino, A., Kubistin, D., Martinez, M., Rudolf, M., Harder, H., Berresheim, H., Elste, T., Plass-Dülmer, C., Stange, G., and Schurath, U.: Technical Note: Formal blind intercomparison of OH measurements: results from the international campaign HOxComp, Atmos. Chem.

- Phys., 9, 7923–7948, https://doi.org/10.5194/acp-9-7923-2009, 2009
- Setokuchi, O.: Trajectory calculations of OH radical- and Cl atom-initiated reaction of glyoxal: atmospheric chemistry of the HC(O)CO radical, Phys. Chem. Chem. Phys., 13, 6296–6304, https://doi.org/10.1039/C0CP01942A, 2011.
- Silva, G. D., Graham, C., and Wang, Z.-F.: Unimolecular β-Hydroxyperoxy Radical Decomposition with OH Recycling in the Photochemical Oxidation of Isoprene, Environ. Sci. Technol., 44, 250–256, https://doi.org/10.1021/es900924d, 2010.
- Stone, D., Evans, M. J., Edwards, P. M., Commane, R., Ingham, T., Rickard, A. R., Brookes, D. M., Hopkins, J., Leigh, R. J., Lewis, A. C., Monks, P. S., Oram, D., Reeves, C. E., Stewart, D., and Heard, D. E.: Isoprene oxidation mechanisms: measurements and modelling of OH and HO<sub>2</sub> over a South-East Asian tropical rainforest during the OP3 field campaign, Atmos. Chem. Phys., 11, 6749–6771, https://doi.org/10.5194/acp-11-6749-2011, 2011.
- Tan, D., Faloona, I., Simpas, J. B., Brune, W., Shepson, P. B., Couch, T. L., Sumner, A. L., Carroll, M. A., Thornberry, T., Apel, E., Riemer, D., and Stockwell, W.: HO<sub>X</sub> budgets in a deciduous forest: Results from the PROPHET summer 1998 campaign, J. Geophys. Res., 106, 24407–24427, https://doi.org/10.1029/2001jd900016, 2001.
- Tan, Z., Fuchs, H., Lu, K., Hofzumahaus, A., Bohn, B., Broch, S., Dong, H., Gomm, S., Häseler, R., He, L., Holland, F., Li, X., Liu, Y., Lu, S., Rohrer, F., Shao, M., Wang, B., Wang, M., Wu, Y., Zeng, L., Zhang, Y., Wahner, A., and Zhang, Y.: Radical chemistry at a rural site (Wangdu) in the North China Plain: observation and model calculations of OH, HO<sub>2</sub> and RO<sub>2</sub> radicals, Atmos. Chem. Phys., 17, 663–690, https://doi.org/10.5194/acp-17-663-2017, 2017.
- Wegener, R., Brauers, T., Koppmann, R., Rodríguez Bares, S., Rohrer, F., Tillmann, R., Wahner, A., Hansel, A., and Wisthaler, A.: Simulation chamber investigation of the reactions of ozone with short-chained alkenes, J. Geophys. Res.-Atmos., 112, D13301, https://doi.org/10.1029/2006JD007531, 2007.
- Whalley, L. K., Edwards, P. M., Furneaux, K. L., Goddard, A., Ingham, T., Evans, M. J., Stone, D., Hopkins, J. R., Jones, C. E., Karunaharan, A., Lee, J. D., Lewis, A. C., Monks, P. S., Moller, S. J., and Heard, D. E.: Quantifying the magnitude of a missing hydroxyl radical source in a tropical rainforest, Atmos. Chem. Phys., 11, 7223–7233, https://doi.org/10.5194/acp-11-7223-2011, 2011.
- Whalley, L. K., Blitz, M. A., Desservettaz, M., Seakins, P. W., and Heard, D. E.: Reporting the sensitivity of laser-induced fluorescence instruments used for HO<sub>2</sub> detection to an interference from RO<sub>2</sub> radicals and introducing a novel approach that enables HO<sub>2</sub> and certain RO<sub>2</sub> types to be selectively measured, Atmos. Meas. Tech., 6, 3425–3440, https://doi.org/10.5194/amt-6-3425-2013, 2013.
- Wolfe, G. M., Thornton, J. A., Bouvier-Brown, N. C., Goldstein, A. H., Park, J.-H., McKay, M., Matross, D. M., Mao, J., Brune, W. H., LaFranchi, B. W., Browne, E. C., Min, K.-E., Wooldridge, P. J., Cohen, R. C., Crounse, J. D., Faloona, I. C., Gilman, J. B., Kuster, W. C., de Gouw, J. A., Huisman, A., and Keutsch, F. N.: The Chemistry of Atmosphere-Forest Exchange (CAFE) Model Part 2: Application to BEARPEX-2007 observations, Atmos. Chem. Phys., 11, 1269–1294, https://doi.org/10.5194/acp-11-1269-2011, 2011a.

- Wolfe, G. M., Thornton, J. A., McKay, M., and Goldstein, A. H.: Forest-atmosphere exchange of ozone: sensitivity to very reactive biogenic VOC emissions and implications for incanopy photochemistry, Atmos. Chem. Phys., 11, 7875–7891, https://doi.org/10.5194/acp-11-7875-2011, 2011b.
- Wolfe, G. M., Cantrell, C., Kim, S., Mauldin III, R. L., Karl, T., Harley, P., Turnipseed, A., Zheng, W., Flocke, F., Apel, E. C., Hornbrook, R. S., Hall, S. R., Ullmann, K., Henry, S. B., Di-Gangi, J. P., Boyle, E. S., Kaser, L., Schnitzhofer, R., Hansel, A., Graus, M., Nakashima, Y., Kajii, Y., Guenther, A., and Keutsch, F. N.: Missing peroxy radical sources within a summertime ponderosa pine forest, Atmos. Chem. Phys., 14, 4715–4732, https://doi.org/10.5194/acp-14-4715-2014, 2014.